Radiophysics and Quantum Electronics, Vol. 53, No. 11, April, 2011
(Russian Original Vol. 53, No. 11, November, 2010)

ARTIFICIAL PERIODIC IRREGULARITIES, HYDRODYNAMIC INSTABILITIES, AND DYNAMIC PROCESSES IN THE MESOSPHERE — LOWER THERMOSPHERE

N. V. Bakhmet'eva,* G. I. Grigor'ev, and A. V. Tolmacheva

UDC 551.510.536

We present the results of measuring characteristics of the ionosphere and neutral atmosphere by the method of resonant scattering of radio waves by artificial periodic irregularities of the ionospheric plasma in the altitude range 90–120 *km. It is shown that the altitude–time variations of the measured characteristics are in many respects stipulated by the propagation of atmospheric waves. Hydrodynamic instabilities in the mesosphere — lower thermosphere are analyzed. Criteria of development of different-type instabilities are presented. Contribution of different processes to the dynamics of the medium is estimated on the basis of the measurement results.*

1. INTRODUCTION

The physical parameters describing the Earth's ionosphere state vary both in space and time. This also concerns the mesosphere — lower thermosphere altitudes at which significant variations in the temperature, density, and velocity of the neutral component take place [1]. The dynamics of the atmosphere at these altitudes determines in many respects the pattern of its state and influences the energy exchange between the lower and upper layers [2].

One of the effective methods of studying the dynamic phenomena in the upper atmosphere is the method of resonant scattering of radio waves by artificial periodic irregularities of the ionosopheric plasma [3]. Long-term measurements of characteristics of the ionosphere and neutral atmosphere at altitudes 90–120 km, which were performed by this method in 1990–1992, showed that the wave motions with periods from 10–15 min to a few hours distinctly manifest themselves in temporal variations in the amplitude, phase, and relaxation time of the signal scattered by artificial periodic irregularities, as well as in variations in the temperature, density, and vertical velocity of the plasma. The results of the vertical plasma velocity measurements in February–March 1999 can be used as the example. Figure 1, which was taken from [3], presents temporal variations in the vertical plasma velocity dated February 27, 1991. Figure 1*a* shows the minute (average minute) variations in the plasma velocity with a characteristic period of 30–40 min and an approximating curve which yields a longer-variation period of about 6 h. Figure 1*b* presents only the approximating curves for six altitudes characterizing long variations, which illustrate the altitude tranformation of a large-scale perturbation.

Wave motions also influence altitude–time variations in the electron number density. Figure 2, which is also taken from [3], shows, in terms of isolines of the electron number density, its wave-like variations, as well as the unstable nature of the interlayer valley between the E and F layers. Later, the presented results were employed for modeling of characteristics of the internal gravity waves on the basis of the linear theory of their free propagation in an unbounded isothermal unperturbed atmosphere [4, 5]. By measured

* nbakh@nirfi.sci-nnov.ru

Radiophysical Research Institute, Nizhny Novgorod, Russia. Translated from Izvestiya Vysshikh Uchebnykh Zavedenii, Radiofizika, Vol. 53, No. 11, pp. 695–711, November 2010. Original article submitted November 24, 2010; accepted December 20, 2011.

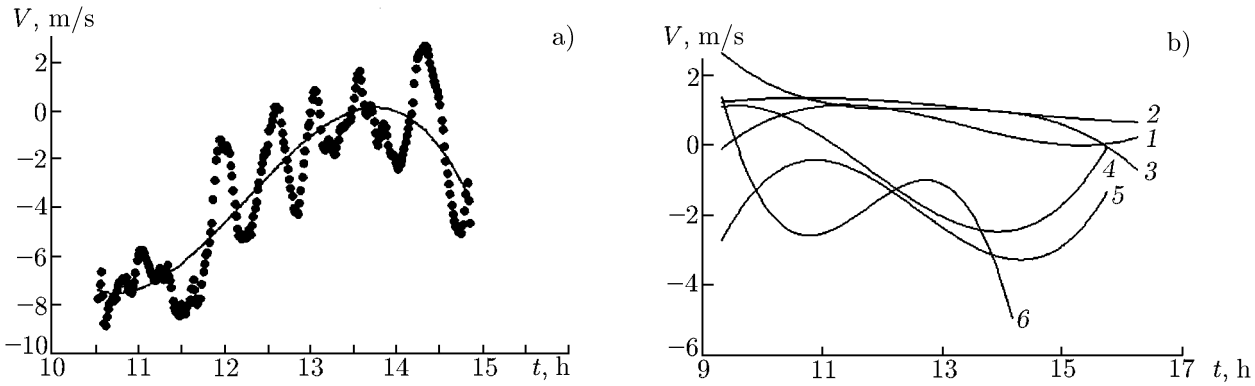

Fig. 1. Time dependence of the vertical velocity of the plasma at an altitude of 117 km, which was obtained in the measurements by the method of artificial periodic irregularities in February 27, 1991. On panel (*a*), the dots correspond to the minute values and the smoothed curve characterizes the larger fluctuations. Panel (*b*) shows the smoothed altitude–time variations in the vertical velocity for six altitudes from 97 km (curve *1*) to 117 km (curve *6*) with 5-km interval for December 6, 1991.

variations in the vertical velocity, we determined the dominant periods and amplitudes of wave motions. Then, using the polarization relationships for internal gravity waves, we calculated the relative amplitudes of the atmospheric temperature and density for the waves with periods of 15 min to 4 h propagating in the atmosphere. It was shown that a satisfactory agreement of the measured values and calculation results in the mentioned approximation took place only for short-period waves with a period of 15–30 min. In a number of cases, the amplitude of quasiperiodic oscillations of measured parameters increased with time and altitude, which can be evidence for the unstable propagation of the waves or the development of hydrodynamic instabilities in the medium.

In recent years, for a study of the mesosphere — lower thermosphere, the method of creating artificial periodic irregularities at two frequencies (with two spatial scales) [6] was used and a large volume of results of measuring the electron number density, vertical velocity, temperature, and density of the atmosphere at the altitudes of the E region was obtained. The velocities of turbulent motions at altitudes lower than the turbopause were also determined. On the basis of these data, the dynamic phenomena which could affect the sort of the altitude–time variations of the parameters of the ionosphere and neutral atmosphere were analyzed. The propagation of internal gravity waves and their influence on the artificial periodic structure, as well as the instability of the medium due to the wave action are important factors. In this paper, we present the data on temperature and density of the neutral atmosphere and velocities of regular vertical and turbulent motions based on the measurements performed in April 2006 and in September 2007. Hydrodynamic instabilities in the mesosphere — lower thermosphere have been analyzed. Criteria of the appearance of instabilities of different types are presented. Numerical estimates of the contribution of different processes to the dynamics of the medium are made on the basis of the measurement results.

2. METHOD OF DETERMINING CHARACTERISTICS OF THE IONOSPHERE AND NEUTRAL ATMOSPHERE AND THE MEASUREMENT RESULTS

The methods of measuring atmospheric parameters by means of resonant scattering of radio waves by artificial periodic irregularities are described in detail in [3, 7–9]. They were developed as the effect of high-power high-frequency radio waves on the ionosphere was studied. The interference of the radio waves incident on and reflected from the ionosphere in such an effect gives rise to a standing wave. A periodic structure of the electron-density disturbances is formed in the field of the standing wave. Artificial periodic irregularities arise in an altitude interval of from about 60 km to the point of reflection of the high-power radio wave from the ionosphere. Resonant (Bragg) scattering from the scattering region where the

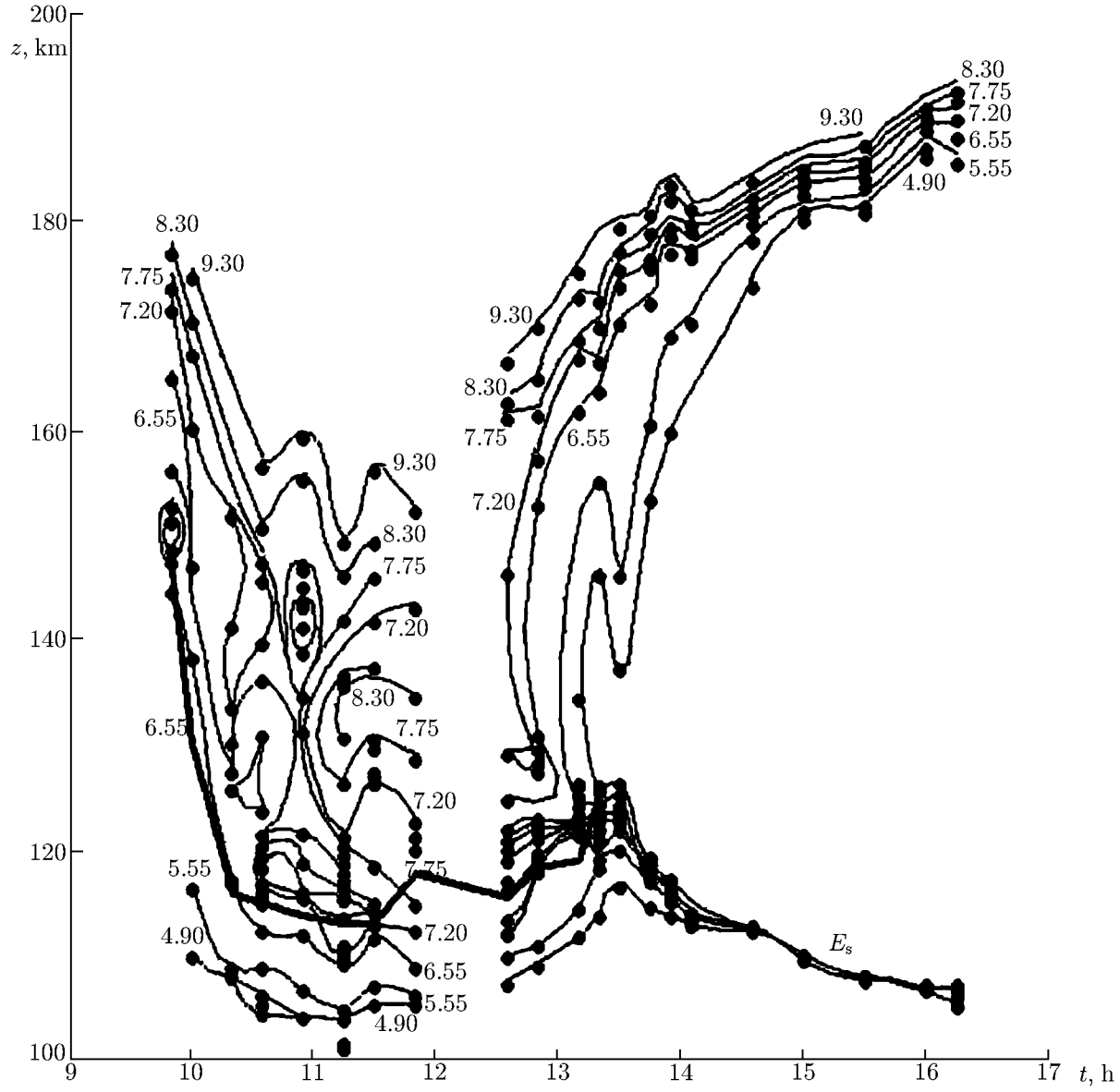

Fig. 2. Isolines of the electron number density in the altitude–time coordinates in units of 10^{-4} cm^{-3} (the values are given near the isolines) for December 17, 1991. The bold line shows the height of the E-region maximum [3].

wavelengths of the perturbing and probing waves are equal occurs when the artificial periodic irregularities are sounded by high-frequency radio pulses. Amplitudes and phases of the scattered signals are recorded at the time of relaxation of the irregularities after the effect of high-power radio waves on the ionosphere is stopped.

Altitude and time dependencies of the amplitudes and phases of scattered signals give information on different parameters of the ionospheric plasma and atmosphere. The largest volume of information can be obtained for the ionospheric E region. These are the data on the electron number density, temperature, and density of the neutral atmosphere, vertical velocity, etc. [3]. Using the obtained data on ionospheric and atmospheric parameters in the ionospheric E region, one can study the dynamics of the medium, including the ionization inhomogeneities, e.g., sporadic layers, and determine characteristics of the wave motions and natural turbulence of the lower ionosphere [10]. In the E region (90–130 km), artificial periodic irregularities are formed due to the diffusional redistribution of the plasma. Their spatial scale in altitude is equal to the

wavelength Λ of the standing wave. The relaxation of artificial irregularities after the cancellation of the high-power impact occurs during the ambipolar diffusion with the diffusional time of relaxation

$$\tau = (K^2 D_\mathrm{a})^{-1}, \tag{1}$$

where $K = 2\pi/\Lambda$, D_a is the ambipolar diffusion coefficient, $\Lambda = \lambda_0/(2n)$, λ_0 is the wavelength of the perturbing wave in vacuum, and n is the refractive index of the wave, which depends on its frequency and the plasma density. The ambipolar diffusion coefficient is determined by characteristics of the ambient medium, namely, the electron T_e and ion T_i temperatures and the ion–molecule collision frequency ν_im:

$$D_\mathrm{a} = \frac{\kappa\,(T_\mathrm{e} + T_\mathrm{i})}{M_\mathrm{i}\nu_\mathrm{im}}, \tag{2}$$

where κ is the Boltzmann constant and M_i is the ion mass. We now consider briefly the diagnostic techniques employed for the E region.

2.1. Method of measuring the atmospheric temperature and density

This method was described by us earlier and is given in ample detail in [3, 11]. The main results obtained by this method during the creation of a periodic structure at one frequency are presented in [12, 13].

The temperature and density values in the locally isothermal approximation and under the condition $T_\mathrm{e} = T_\mathrm{i} = T$ are determined as follows:

$$T = MgH/\kappa, \qquad \rho(z) = \frac{8K^2\kappa T\tau(z)}{\beta}\,\frac{M}{M_\mathrm{i}}. \tag{3}$$

Here, M_i and M are the average masses of ions and molecules, respectively, H is the altitude of the uniform atmosphere, $\nu_\mathrm{im} = \beta\rho/M$, and β is the proportionality coefficient, which has the value $\beta = 0.38 \cdot 10^{-16}\ m^3/s$ [3]. From Eqs. (1) and (2) it follows that the relaxation time of artificial periodic irregularities depends not only on the atmospheric parameters, but also, via the refractive index of the standing wave, on the electron number density.

The described method of determining the atmospheric temperature and density is employed in the following way. The initial altitude is chosen from the measured altitude dependence of the relaxation time $\tau(z)$. The atmosphere is assumed locally isotermal in a small altitude interval. Then the altitude of the uniform atmosphere is found from the dependence $\tau(z)$ and the temperature and density of the neutral atmosphere at a particular altitude is found from Eqs. (3). Then the procedure is repeated with the transition to the higher levels, which yields the profiles $T(z)$ and $\rho(z)$. By virtue of the adopted locally isothermal approximation, the method of determining atmospheric parameters is good for gradual variations of the ionospheric and atmospheric parameters with altitude: under such conditions, the measurement errors do not exceed 10% for the temperature and 15% for the density. If the temperature determination error was more than 15–20%, then the data were assumed unreliable and were rejected.

2.2. Two-frequency method of determining characteristics of the ionosphere and neutral atmosphere at the altitudes of the E region

This method is based on the creation of artificial periodic irregularities by means of the radiation of high-power radio waves at two frequencies separated by 1 MHz. In this case, periodic structures with two different spatial scales are created [6, 7]. The irregularities are sounded by probing radio waves at the same frequencies, and at each frequency their relaxation times are determined from the e-fold decrease in the scattered-signal amplitude. Since the parameters of the undisturbed medium at a particular altitude do not depend on the impact frequency, the ratio $\theta = \tau_1/\tau_2$ of the relaxation times of scattered signals measured at two frequencies is a function of altitude and is determined unambiguously by these frequencies,

the electron gyrofrequency, and the electron number density. The electron number density $N(z)$ is found from the quantity $\theta(z)$. After the refractive indices of the waves are calculated at each operating frequency, the atmospheric temperature and density as functions of the altitude are determined.

2.3. Method of determining the velocity of the vertical plasma motion

The velocity V_z of the vertical plasma motion, which coincides, up to the altitude 120–130 km, with the velocity of the neutral component since the plasma of the lower ionosohere is a minority in the neutral medium [14], is determined by measuring the phase of the signal scattered by artificial periodic irregularities [3]. Temporal variations φ of the scattered-signal phase are approximated by the linear dependence $\varphi(t) = \varphi_0 + bt$, where $b = 4\pi V_z/\lambda$, λ is the wavelength of the high-power wave in the medium, $V_z = (\lambda/4\pi)\,\mathrm{d}\varphi/\mathrm{d}t$. The positive values of the velocity correspond to the downward motion. Since in the E region and for the operating frequencies 4.7 and 5.6 MHz the refractive index n, as calculations of the electron-density profile show, differs only slightly from unity, the corrections introduced by its allowance into the velocity amount to no more than 10–15% towards its increase. This fact does not affect the altitude–time variations of the vertical velocity.

2.4. Turbulent velocity

The vertical component of the turbulent velocity is determined by the difference of the relaxation time from its diffusional value. The point is that the small-scale motion stipulated by the turbulence affects the characteristics of the signal scattered by artificial periodic irregularities since it disturbs their ordered structure. Turbulent motion leads to a dephasing of the signals scattered by different parts of the scattering volume, which in a natural way causes a decrease in the received-signal amplitude and a broadening of its angular spectrum. The relaxation time of the scattered signal decreases compared with the diffusional signal under the action of turbulence. The two-frequency method of creating artificial periodic irregularities and recording of scattered signal permits one to use the expression

$$V_\mathrm{t} = \left(\frac{K_1}{K_2\tau_2} - \frac{K_2}{K_1\tau_1}\right) \Big/ (K_1 - K_2) \tag{4}$$

for the turbulent velocity. Here, $K_1 = 4\pi/\lambda_1$, $K_2 = 4\pi/\lambda_2$, and τ_1 and τ_2 are the relaxation times of the scattered signal at each frequency [3].

To determine the turbulent velocity, the measured profile of the electron number density and the relaxation times at two frequencies are used. By the altitude profile of the turbulent velocity $V_\mathrm{t}(h)$ one can estimate the turbopause altitude, i.e., the altitude at which the coefficients of the ambipolar and turbulent diffusion become equal and the turbulent velocity decreases almost down to zero.

2.5. Results of determining the atmospheric characteristics during the creation of artificial periodic irregularities at two frequencies

In this paper, we discuss the results of the measurements of atmospheric characteristics by the two-frequency method, which were performed in April 2006 and September 2007 on the basis of the "Sura" heating facility of the Radiophysical Research Institute (56.1°N, 46.1° E). Two transmitters of the facility were operated at a frequency of 4.7 MHz, and the third one, at a frequency of 5.6 MHz with effective powers 70 and 15 MW, respectively. The transmitters were operated alternately at each frequency in cycles of 15-s duration. Each cycle started with the continuous operation of the transmitter for 3 s, and then a 12-s pause followed. During the pause, pulses with a duration of 30 μs and a repetition rate of 50 Hz were radiated. In the odd cycles, the transmitters were operated at a frequency of 4.7 MHz and in the even cycles, at a frequency of 5.6 MHz. The scattered signals were received by means of the setup for a study of the ionosphere by the partial-reflections technique. The altitude recording step amounted to 1.4 km. The

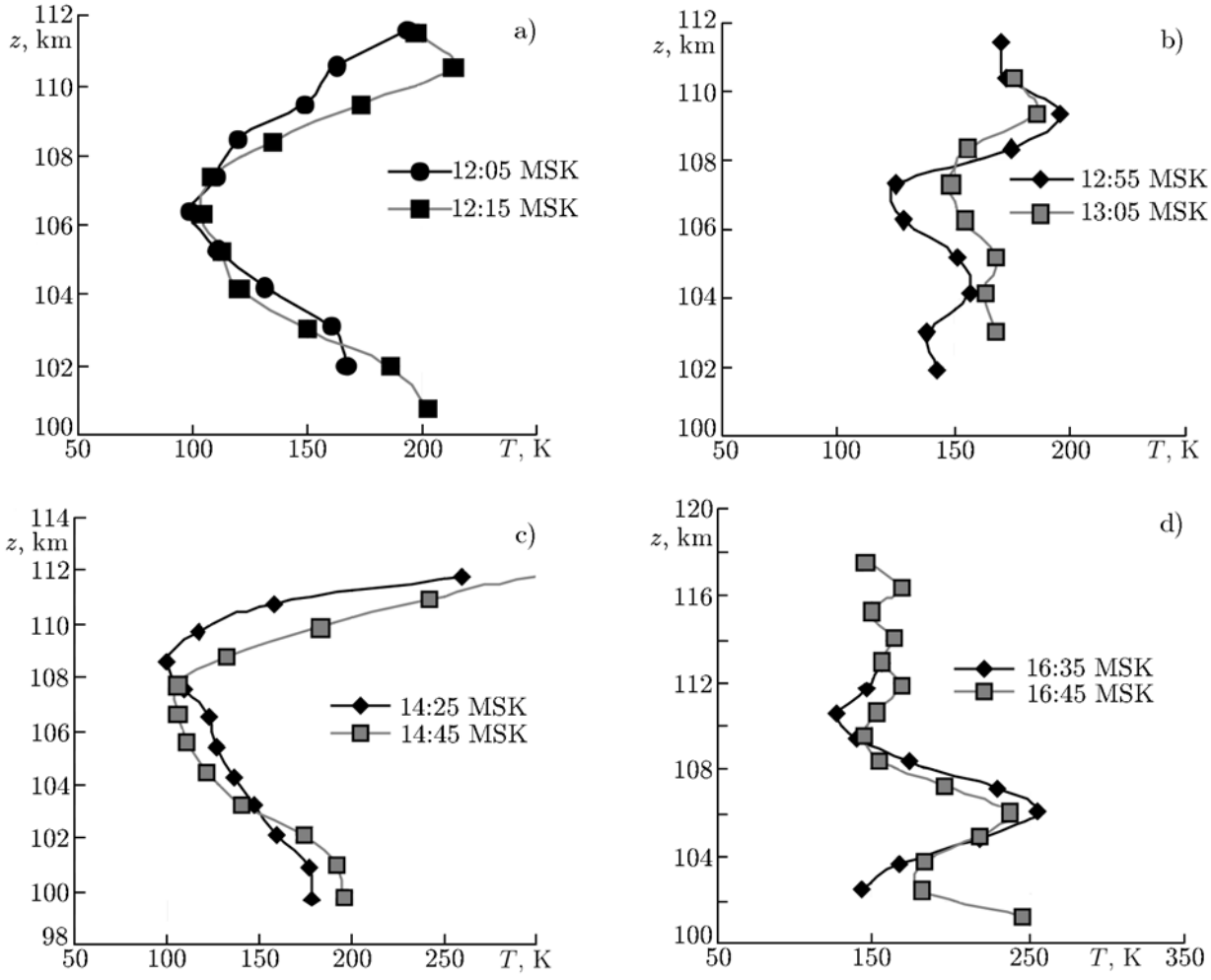

Fig. 3. Altitude profiles of the neutral-component temperature for several successive measurement sessions in April 4, 2006.

signals were recorded for 6 s after the continuous radiation of the facility transmitters was switched on. This time was sufficient for the complete relaxation of irregularities. The measurements were performed in the daytime period for a few hours. At each altitude, the amplitude A and phase φ of the signals scattered by artificial periodic irregularities were measured and the relaxation times τ were determined. To decrease the statistical error when the electron number density is determined, the individual values of the relaxation times were averaged at each altitude over 10–20 samples (for 5–10 min). The altitude profiles of the temperature and density of the neutral atmosphere were determined according to Eq. (3). Figure 3 shows examples of the $T(z)$ profiles for April 4, 2006. Figures 3*a* and 3*c* show typical smooth, "quiet" profiles with the minimum temperature at an altitude of 106–108 km.[1] Figures 3*b* and 3*d* show the "unperturbed" temperature profiles which appeared in the subsequent periods of time, namely, in the sessions 12:55–13:05 MSK in Fig. 3*b* and 16:35–16:45 MSK in Fig. 3*d*. Such perturbations disappeared with the time and then could appear again. A similar behavior of $T(z)$ was observed in the experiments as well. For example, Fig. 4 shows the $T(z)$ profile with the same features for September 24, 2010.

By the lower branch of the "quiet" temperature profile, we determined the negative gradient $\mathrm{d}T/\mathrm{d}z$ with $T(z)$ approximation by a linear function. The obtained quantity $\mathrm{d}T/\mathrm{d}z$ amounted to $-(17–20)$ K/km for April 4, 2006 and was of the order of -25 K/km for the profiles obtained in September 24, 2007. Figure 4*b*

[1] Note that the minimum temperature can be stipulated by the atmospheric-parameter variations caused by the propagation of internal gravity and tidal waves.

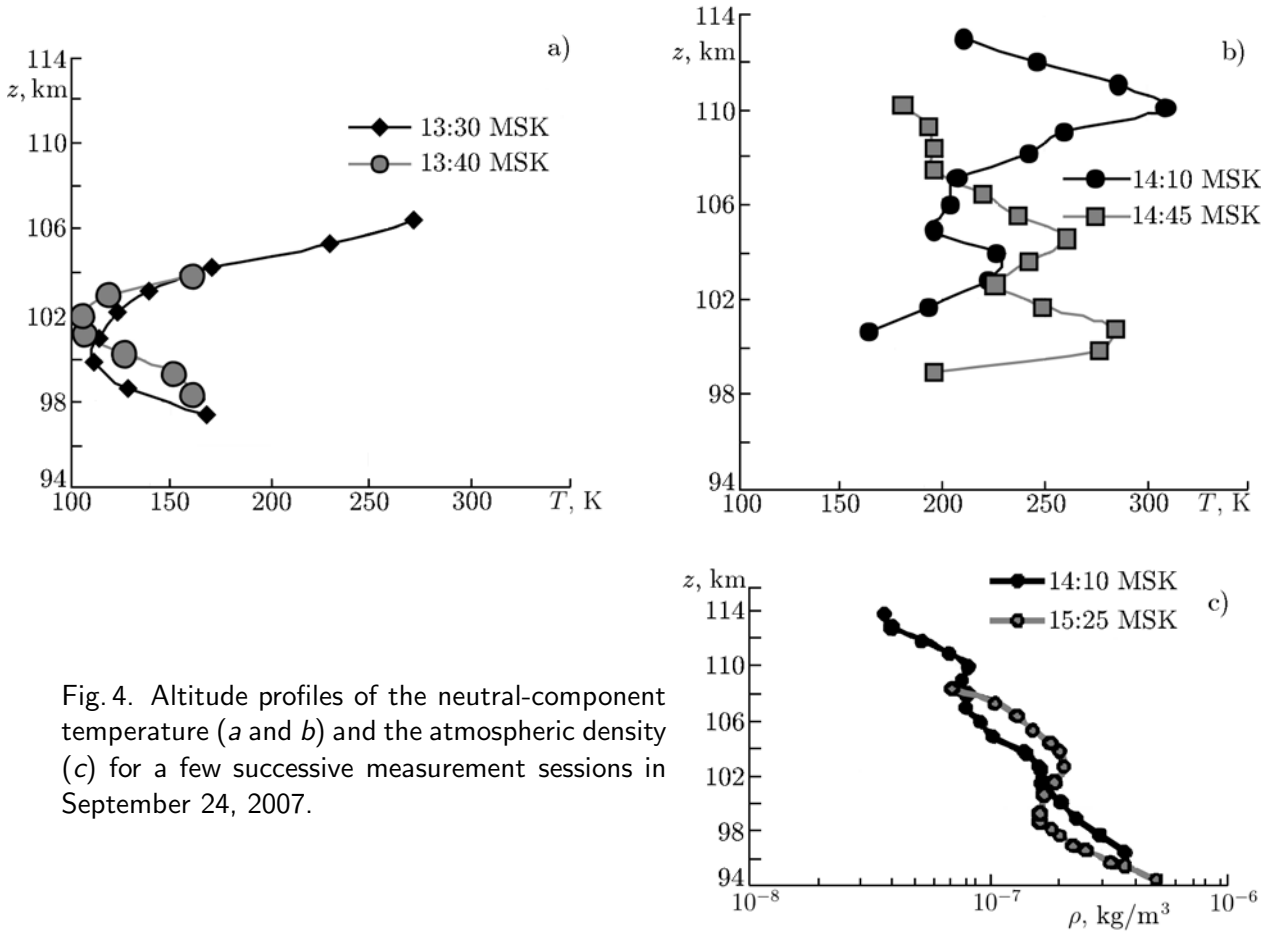

Fig. 4. Altitude profiles of the neutral-component temperature (*a* and *b*) and the atmospheric density (*c*) for a few successive measurement sessions in September 24, 2007.

shows the perturbations which appeared at 14:10 and 14:45 and significantly enhanced later at 15:15 and 15:25 MSK. In Fig. 4*c* showing the altitude dependencies of the density $\rho(z)$ for 14:10 and 15:25 MSK it is seen that the oscillation amplitude increases at 15:25 compared with 14:10.

The vertical velocities were determined in the case where the time dependence of the scattered-signal phase was approximated well by a linear function. This was not always possible for technical (instrumental) reasons. For example, the vertical-velocity data for April 4, 2006 were not obtained. The results of measuring V_z in the experiment of September of 2007 were discussed in detail in [15]. It was noted, in particular, that the spread of the velocity variations was the least in the altitude intervals 60–80 and 95–110 km and drastically increased at altitudes 85–90 km due to the turbulence effect. Figre 5 shows plots of the temporal variation of the vertical velocity, amplitude, and relaxation time of the scattered signal at the altitude $z = 100$ km, which were smoothed out by the sliding-mean technique for 6 min. It is seen, especially in the amplitude and velocity plots, that their oscillations in separate intervals of time are enhanced, and on the whole these times correspond to those presented in the temperature profiles of Figs 4*a* and 4*b*. The enhancement of oscillations is also seen in the altitude profiles of the vertical velocity for the sessions at 14:45 MSK and 15:15 MSK shown in Fig. 6. It is seen, firstly, that the waves propagate in the studied altitude interval and, secondly, the velocity oscillation amplitude in the session of 15:15 MSK strongly increases, which indicates that the amplitude of the internal gravity waves increase and, possibly, an instability develops.

The turbulent velocities were estimated according to Eq. (4). For this purpose, we used the relaxation times of the scattered signal at frequencies 4.7 and 5.6 MHz and calculated the altitude profile of the electron number density $N(z)$ on the basis of the ratio of these times $\theta = \tau_1/\tau_2$. The estimates yielded fairly high values of the turbulent velocity up to 7–10 m/s at altitudes lower than the turbopause altitude by 5–10 km. It is found that the height 100–105 km was the most probable altitude of the turbopause for the Fall 2007.

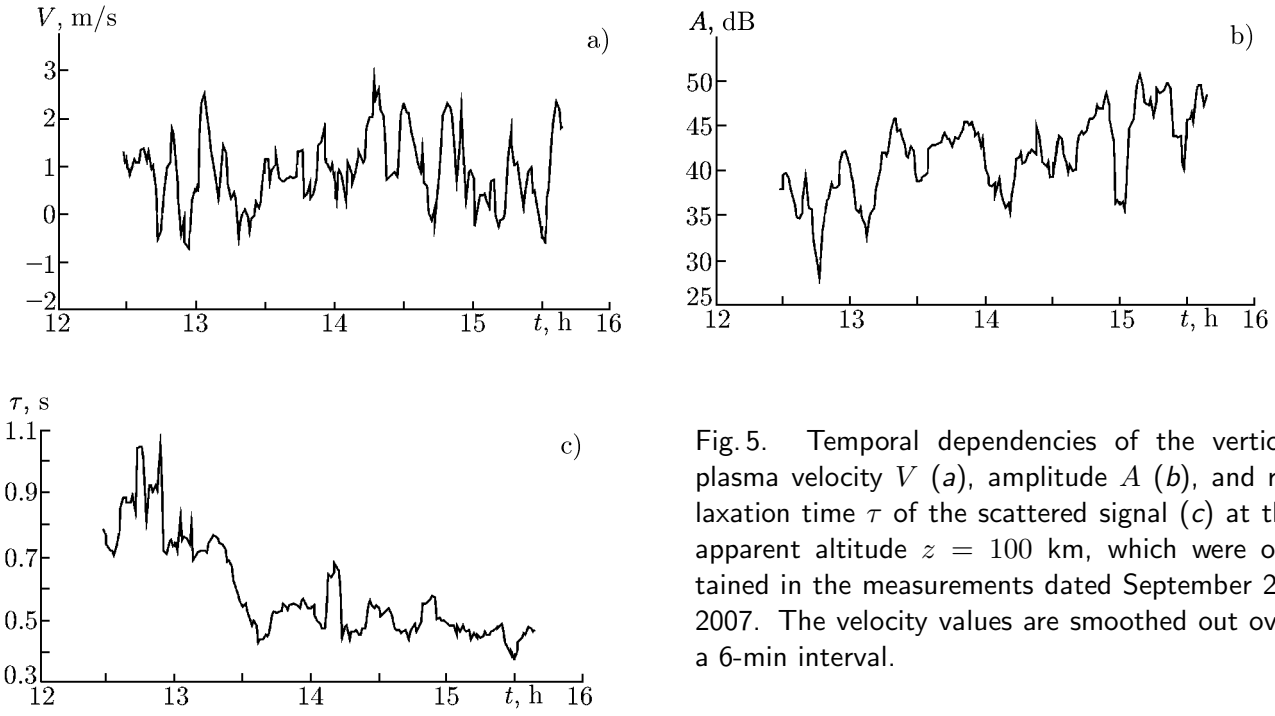

Fig. 5. Temporal dependencies of the vertical plasma velocity V (*a*), amplitude A (*b*), and relaxation time τ of the scattered signal (*c*) at the apparent altitude $z = 100$ km, which were obtained in the measurements dated September 24, 2007. The velocity values are smoothed out over a 6-min interval.

3. ATMOSPHERIC GRAVITY WAVES AND THE PROBLEMS OF HYDRODYNAMIC STABILITY. BASIC RELATIONSHIPS

It was shown in Sec. 2 that in the analysis of the mesospheric dynamic processes by means of artificial periodic irregularities, one has to allow for the influence of internal gravity waves on the periodic structure (see also [3]). Near the mesopause, the estimated densities of the energy flux transmitted by these waves range from several to a few hundreds $\mathrm{erg} \cdot \mathrm{cm}^{-2} \cdot \mathrm{s}^{-1}$, which is comparable with the flux density of the Sun's high-frequency radiation (of the order of $10\ \mathrm{erg} \cdot \mathrm{cm}^{-2} \cdot \mathrm{s}^{-1}$) [2]. Hydrodynamic instabilities play an important role in the dynamics of the lower ionosphere. Consider the hydrodynamic instabilities which can affect the atmospheric-parameter variations.

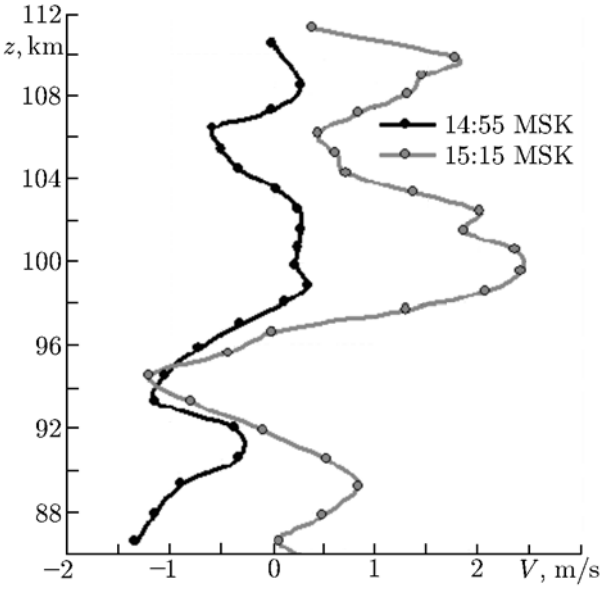

Fig. 6. Altitude profiles of the vertical velocity in the sessions at 14:55 and 15:15 MSK in September 24, 2007.

3.1. Isothermal atmosphere

In an isothermal atmosphere, the particle oscillations of the medium are stable. If a particle of mass M_0 at altitude z is singled out in the atmosphere with the density $\rho_0(z)$ and is displaced by ζ from the equilibrium position, then, being unaffected, it will perform oscillations under the action of the gravity and Archimedean forces. These oscillations are described by the equations [16]

$$\frac{\partial^2 \zeta}{\partial t^2} + \omega_g^2 \zeta = 0, \tag{5}$$

$$\omega_g^2 = -g\left(\frac{1}{\rho_0}\frac{\partial\rho_0}{\partial z} + \frac{g}{c_\mathrm{s}^2}\right), \tag{6}$$

where ω_g is the Brunt–Väisälä frequency, g is the free-fall acceleration, and c_s is the sound speed. For the model of an isothermal atmosphere ($T_0 = \mathrm{const}$), in which the equilibrium pressure p_0 and density ρ_0 vary exponentially $p_0/p_\mathrm{s} = \rho_0/\rho_\mathrm{s} = \exp(-z/H)$, where $H = \kappa T_0/(Mg)$ is the altitude scale of a uniform atmosphere, from Eq. (6) we obtain an expression for the Brunt–Väisälä frequency in the form $\omega_g^2 = (\gamma-1)\,g^2/c_\mathrm{s}^2$. In this case, $\omega_g^2 > 0$, and the numerical value of the frequency ω_g for the heat–capacitance ratio $\gamma = 1.4$, $g = 10$ m/s^2 and $H = 8$ km is equal to $\omega_g \approx 1.7\cdot 10^{-2}\ s^{-1}$ (the period corresponding to this frequency is equal to $T_g = 2\pi/\omega_g \approx 6$ min).

3.2. Atmosphere with a linear temperature profile

For another model of the neutral atmosphere, in which the temperature linearly varies with the altitude z,

$$T_0(z) = T_\mathrm{s}\,(1+\alpha z), \tag{7}$$

where $\alpha = \mathrm{const}$, and the density $\rho_0(z)$ and the pressure $p_0(z)$ are determined by the formulas

$$\rho_0(z) = \rho_\mathrm{s}\,(1+\alpha z)^{-(\eta+1)}, \qquad p_0(z) = p_\mathrm{s}\,(1+\alpha z)^{-\eta}, \tag{8}$$

where T_s, P_s, and ρ_s are the constants, $c^2 = c_\mathrm{s}^2\,(1+\alpha z)$ is the sound speed, $\eta = 1/(\alpha H_\mathrm{s})$, and the subscript s characterizes the quantities for $z = 0$ ($H_\mathrm{s} = \kappa T_\mathrm{s}/(Mg)$). Under these conditions, for ω_g^2 we obtain from Eq. (6) the relationsip

$$\omega_g^2 = \frac{g}{1+\alpha z}\left(\alpha + \frac{\gamma-1}{\gamma H_\mathrm{s}}\right). \tag{9}$$

It follows from Eqs. (5) and (9) that oscillations of an air particle with mass M_0 can increase in time if the temperature of the medium decreases with the altitude, i.e., α is negative. In this case, the instability development condition

$$|\alpha| > \alpha_\mathrm{s} = \frac{\gamma-1}{\gamma H_\mathrm{s}} \tag{10}$$

should be fulfilled. At an altitude of 80–85 km (the altitude of the mesopause), the numerical value of α_s for $\gamma = 1.4$ and $H_\mathrm{s} = 5$ km ($T_\mathrm{s} = 175$ K) is equal to $\alpha_\mathrm{s} \approx 5.7\cdot 10^{-2}$ km^{-1}, which corresponds to the adiabatic temperature gradient $\partial T_0/\partial z = \alpha_\mathrm{s} T_\mathrm{s} \approx -10\ K\cdot\mathrm{km}^{-1}$. For other T_s and H_s, the values α_s are easily determined by Eq. (10). For example, at the altitudes of the lower thermosphere 110–120 km, for $H_\mathrm{s} = 10$ km ($T_\mathrm{s} = 350$ K) we obtain $\alpha_\mathrm{s} \approx 2.85\cdot 10^{-2}$ km^{-1}.

Thus, if the temperature decreases more rapidly in some interval of altitudes in the atmosphere than it follows from Eq. (7), then any perturbations (including the internal gravity waves) rise with the time. This means that we can speak of instability of the medium to these perturbations. The linear profile of the temperature is a certain idealization. The dispersion equation of internal gravity waves and analysis of their stability for the more real piecewise-linear dependence $T(z)$ are given in [17]. In the case where the equilibrium temperature of the atmosphere is specified by a linear function of altitude, the wave equation for internal gravity waves reduces to a hypergeometric one. In [17], analytical expressions for the perturbation fields are found and a characteristic equation, whose solution allowed the dispersion characteristics to be determined at a frequency close to the Brunt–Väisälä frequency, was obtained. A detail analysis of the characteristic equation in [17] is performed for larger horizontal wave scales compared with the layer thickness. Numerical analysis of the characteristic equation for given horizontal wave numbers permits one to find the dependence $\omega(k)$ on the entire plane of complex frequencies and specify the conditions of stability of the obtained solution relative to the temperature gradient and other parameters of the problem. The results of numerical analysis of the characteristic equation are presented in [17] for the negative gradient

$(\alpha H_s)^{-1} = -3.3$ and the layer height $z = 1.2H_s$. Finally, we obtain the complex frequencies as functions of the horizontal wave numbers. It is found that the frequencies $\omega_1 = 0.835\omega_{gs}$ and $\omega_2 = 0.957\omega_{gs}$ correspond to the stable solutions with $k_1 \approx 2H_s^{-1}$ and $k_2 \approx 5H_s^{-1}$.

3.3. Stratification of horizontal wind

Another factor leading to the instability of the atmospheric perturbations is the presence of horizontal wind motions dependent on altitude. In this case, it is important to allow for the altitude velocity gradient. The value of the Richardson number, which serves as a criterion of the stable state or possible instability development, should be estimated. For a certain altitude profile of the horizontal wind velocity, when its altitude gradient exists, the so-called shear instability develops [18]. The problem of stability of perturbations in this case can be analyzed in terms of the semi-bounded model of an isothermal atmosphere with the density $\rho_0(z) = \rho_s \exp(-z/H)$ and a linear profile of the horizontal velocity $u(z) = u_0 z/d$ of the medium, where d is the vertical scale of the horizontal wind velocity. For this case, an equation for the vertical component of the perturbation velocity V_z, which determines its vertical variation, was obtained in [18]. It was assumed that V_z is varied with the time t and along the horizontal coordinate x by the harmonic law

$$V_z \propto \exp(ikx - i\omega t). \tag{11}$$

After some algebra, this equation reduces to the Whittaker equation for the degenerate hypergeometric function $W_{j,m}(\xi)$, for whose indices the designations $j = (1+4k^2d^2)^{-1/2}$ and $m^2 = (1/4) - \mathrm{Ri}$ are used. The Richardson number $\mathrm{Ri} = -(g/\rho_0)\,(\partial\rho_0/\partial z)\,(\partial u_0/\partial z)^{-2}$ for the given problem has the form $\mathrm{Ri} = gd^2/(Hu_0^2)$, and the variable $\xi = [z/d + \omega d/(kHu_0)]\,(1+4k^2H^2)^{1/2}$. The asymptotic behavior of the function $W_{j,m}(\xi)$ at the infinity for $\xi \to \infty$ is determined by the formula $W_{j,m} \approx \xi^j \exp(-\xi/2)$. The boundary condition $V_z = 0$ for $z = 0$ is fulfilled if the expression $\omega d/(kHu_0)\,(1 + 4k^2H^2)^{1/2}$ coincides with the nulls of the function $W_{j,m}(\xi)$. Under the condition $m^2 < 0$, the hypergeometric function $W_{j,m}(\xi)$ has only the real roots $\xi = \xi_n$, for which $W_{j,m}(\xi) = 0$. This means that the requirement $m^2 < 0$, or the condition

$$\mathrm{Ri} > 1/4, \tag{12}$$

which is equivalent to it, is a sufficient condition for stability of the medium with respect to small-amplitude perturbations when the imaginary part of the frequency $\mathrm{Im}\,\omega = 0$. Equation (12) represents the Richardson stability criterion, which is well known in physics. In [19], the same condition of stability was obtained for the shear flows in an inhomogeneous unbounded medium. It has been established in the numerous studies that the stabiility of the shear flows in inhomogeneous media takes place in the case where the local Richardson number always exceeds its critical value $\mathrm{Ri_c} = 1/4$ (see, e.g., [20]).

The physical meaning of Eq. (12) consists in that the stabilizing role of the gravity field and related stratification of the medium dominates the destabilization due to the flow-velocity shear leading to the mixing of the neighboring layers [18]. It can be shown that with the fulfillment of the condition $-g\,\mathrm{d}\rho\,\mathrm{d}z > \rho\,(\mathrm{d}u)^2/4$, i.e., when $\mathrm{Ri} = -(g/\rho_0)\,(\mathrm{d}\rho_0/\mathrm{d}z)\,(\mathrm{d}u/\mathrm{d}z)^{-2} > 1/4$, the shear of the horizontal velocity $\mathrm{d}u/\mathrm{d}z$ is not sufficient for mixing the neighboring layers, i.e., a stability takes place and the medium is stably stratified.

The occurrence of an instability in a stably stratified medium requires that the condition for the Richardson number $\mathrm{Ri} < 1/4$ is fulfilled somewhere inside the interval of the altitude variation of the horizontal velocity $u_0(z)$. In the case where the stability condition is not fulfilled, the index of the perturbation rise due to the shear instability can be estimated by making use of the expression for its growth rate (see the text below).

3.4. Nonstationary motion of the medium

The motion of the medium can be not only nonuniform in space, but also time-dependent. Such a nature of the wind motions leads to a parametric instability of weak perturbations and the generation of

waves. If among the wind-velocity variations $u_0(t)$, one harmonic component is chosen in the form

$$u_0(t) = u_1 + u_2 \sin(\Omega t), \tag{13}$$

then for the periodic (with respect to the deviation coordinates) vertical displacement $\xi \propto \exp(ik_x x + ik_y y - ik_z z + k_0 z)$ one can determine the temporal dependence $\xi(t)$ from the Mathieu equation [21, 22]:

$$\frac{\mathrm{d}^2\xi}{\mathrm{d}\tau^2} + (\delta + \varepsilon\cos\tau)\,\xi = 0, \tag{14}$$

where $\delta = (4k^2\omega_g^2)/[\Omega^2\,(k^2 + k_z^2 + k_0^2)]$, $k^2 = k_x^2 + k_y^2$, $k_0^2 = 1/(4H^2)$, $\tau = \Omega t/2$, and $\varepsilon = [4k_0 k_x u_2\,(k_z - ik_0)]/[\Omega\,(k_x^2 + k_z^2 + k_0^2)]$. The general solution to Eq. (14) can be written in the form [21]

$$\xi(\tau) = D_1 A(\tau)\exp(\mu\tau) + D_2 B(\tau)\exp(-\mu\tau), \tag{15}$$

where D_1 and D_2 are the constants and A_1 and A_2 are periodic functions. Note that for Eq. (14), regions in which stable and exponential, temporally rising solutions for the displacement ξ and other physical characteristics of the atmosphere exist in the (δ, ε) plane. The characteristic index μ determines the stability or instability of the solution. Near the axis $\varepsilon = 0$, the instability arises for the parameter value $\delta = n^2/4$, where n are the integers designating the harmonic numbers. The boundaries of the stability regions for $\varepsilon \ll 1$ are roughly determined by the equalities $\delta = 1/4 \pm \varepsilon/2$. For the internal gravity waves propagating in a medium with horizontal variable wind, this condition yields the following expression for the instability growth rate [21]:

$$\gamma_1 = \mathrm{Re}\,\mu = \frac{u_2}{H}\sin\vartheta\cos\vartheta, \tag{16}$$

where ϑ is the angle determining the direction of the wave vector $\mathbf{k} = (k\sin\vartheta, 0, k\cos\vartheta)$. The ratio of the growth rate γ_1 to the frequency ω of the propagating wave is given by the approximate equality $\gamma_1/\omega \approx (k_0 u_2/\omega_g)\cos\vartheta$. For the chosen values $\vartheta \ll 1$, $u_2 \approx 30$ m/s, $H = 8$ km, and $\omega_g = 1.89 \cdot 10^{-2}$ s^{-1}, we obtain $\gamma_1/\omega \approx 0.2$. Then for the waves with a 30-min period, the instability development time will amount to $\tau_{\mathrm{dev}} \approx 24$ min.[2] The instability development time reduces with decreasing wave period and increasing pulsation component u_2 of the horizontal wind velocity.

Thus, the propagation of internal gravity waves in the atmosphere in the presence of horizontal wind which varies with altitude can be accompanied with their parametric instability. Tidal oscillations of the atmosphere or large-scale propagating waves can be the sources of variable wind [22, 23].

3.5. Additional comments

The conditions of linear stability of the horizontally propagating internal waves of finite amplitude are analyzed in [23]. Using stationary orographic waves as the example, it is shown that such waves are unstable if their amplitude is large enough and their wavelength is small. The critical amplitude for the instability occurrence diminishes as the wavelength squared. To estimate the temporal growth index of the perturbation due to the shear instability, one can make use of the expression for the growth rate γ_1 in the form [24, 25]

$$\gamma_1 \le \max\left[\frac{1}{4}\left(\frac{\partial u_0}{\partial z}\right)^2 - \omega_g^2\right]^{1/2}. \tag{17}$$

For the linear profile of the horizontal velocity $u_0(z) = u_1 + u_2 z/L$, fixed temperature $T_0 = \mathrm{const}$ ($\omega_g = \mathrm{const}$), and the parameter values $u_2 = 50$ m/s, $L = 10^3$ m, and $\omega_g = 2 \cdot 10^{-3}$ s^{-1}, we obtain Ri = 0.16,

[2] Note that the horizontal velocity values $u_2 = 30$ m/s, which were taken for the estimation, are quite real. The results of observation of the sporadic E layer dated September 26, 2010 are presented in [15]. This layer was formed aside the place of recording of artificial periodic irregularities and "passed" through the directivity pattern of the receiving equipment with a horizontal velocity of 20–25 m/s.

i.e, an instability with the growth rate $\gamma_1 \leq 1.5 \cdot 10^{-2}$ s^{-1} takes place, so that the characteristic time of the instability development amounts to a few minutes.

A more detailed discussion of different aspects of the hydrodynamic instability and different-scale wave motion in the atmosphere is contained in monograph [24], in which a survey of theoretical models is given and the results of field experiments are presented.

We also mention that a current instability, which leads to the attenuation of dissipation and a rise in the wave amplitude, is possible when the internal gravity waves propagate at the altitudes of the dynamo region [26]. An instability in the atmosphere can also arise as a consequence of nonlinear effects. For example, it is shown in [27] that the stream jet created by a nonlinear gravity wave can play a siginificant role in the atmospheric instability formation.

We note that the parametric instability in hydrodynamics has an analogy in the case of propagation of electromagnetic waves. An analytical approach to the problems of physics of wave processes in the media with time-dependent dielectric parameteres is considered in [28]. Exact solutions of the Maxwell equations for electromagnetic waves in the model media with a time-varied refractive index are presented there. Both the moving ionization fronts and the nonstationary effects of interaction of electromagnetic waves with the plasma slabs having a variable degree of ionization are considered in that paper.

4. VARIATIONS IN THE CHARACTERISTICS OF A NEUTRAL ATMOSPHERE AND ESTIMATES OF THE PERTURBATION STABILITY

Using the results of measuring the neutral-atmosphere characteristics and a theoretical analysis of the conditions of stability of the medium and the perturbations propagating in it, we make estimates of two types. Firstly, we clarify if the stability condition could, and in which case, be fulfilled in the performed experiments in the case of propagation of internal gravity waves. Secondly, we find out under which conditions the instability characterized by a rise in the variations of parameters (e.g., the neutral-component temperature) could develop when horizontal wind with the vertical shear of velocity exists. We now estimate the Richardson number under conditions of propagation of internal gravity waves by using the characteristic parameter values obtained in the experiment by the method of artificial periodic irregularities, namely, the amplitude of the vertical-velocity variations $V_z = 2$ m/s, the period of internal gravity waves $T_{\rm int} = 30$ min, and the Brunt–Väisälä frequency $\omega_g = 1.7 \cdot 10^{-2}$ s^{-1} (the corresponding period is equal to $T_g \approx 6$ min). The values of the wind velocity shear required for the estimation are absent since the measurement of the horizontal velocity of the neutral component, which is necessary for separated reception of the scattered signal, was not performed. However, with the fulfillment of definite conditions, the horizontal velocity shear can be estimated from the available experimental data. For example, using the truncated dispersion equation of internal gravity waves in the form $\omega^2 \approx \omega_g^2 \lambda_z^2/\lambda_x^2$ [29, 30], where λ_x and λ_z are the horizontal and vertical wavelengths, as well as the condition of incompressibility of the medium $\operatorname{div} \mathbf{V} = 0$, where $\mathbf{V}$ is the total velocity vector, we obtain the expression $u_x \approx -k_z V_z/k_x = -\lambda_x V_z/\lambda_z$ for the horizontal velocity. We determine the horizontal wavelength from the relationship $\lambda_x \approx \lambda_z \omega_g/\omega = \lambda_z T_{\rm int}/T_g$. This relationship is valid when the horizontal wavelength is much greater than the vertical one and the frequency is much smaller than the Brunt–Väisälä frequency [29, 30]. Then for the horizontal velocity shear u, we have the relationship $\mathrm{d}u_x/\mathrm{d}z \approx k_z u_x = 2\pi T_{\rm int} V_z/(\lambda_z T_g)$, and for the Richardson number we obtain the expression $\mathrm{Ri} = \omega_g^2/(\mathrm{d}u_x/\mathrm{d}z)^2 = \lambda_z^2/(V_z T_{\rm int})^2$. For the above-presented values of the vertical wavelength λ_z, the vertical velocity V_z, and the wave period $T_{\rm int}$, we obtain the Richardson number $\mathrm{Ri} = 4$. Hence, the conclusion can be drawn that the propagation of internal gravity waves with a 30-min period in a stably stratified medium does not lead to its instability. Spectral analysis of the temporal variations of the amplitude and relaxation time of the signal scattered by artificial periodic irregularities shows that the waves with half-an-hour and hour periods [15], which, as a rule, are stably recordable, have the largest intensity in the spectrum.

We then present some estimates showing the possibility of the instability development in the medium from the measurement results presented in Sec. 2. Use the temperature altitude profiles (see Figs. 3 and 4). The behavior of the dependence $T(z)$ having a temperature variation part which decreases with the

altitude implies that the instability of the medium develops, and this effect can lead to a drastic variation in the $T(z)$ profile with the time. In Sec. 2, we present the values of the negative altitude profiles $\partial T/\partial z$, determined from the dependence $T(z)$, at an altitude lower than 106–108 km obtained in April 4, 2006 and lower than 100–102 km obtained in September 24, 2007, which varied from -17 K/km to -24 K/km. In Sec. 3.2, it is shown that for the linear profile, the temperature gradient values $\partial T/\partial z < -(10\text{–}12)$ K/km are sufficient for the occurrence of an instability, in accordance with Eqs. (9) and (10). The medium is expected to become turbulent due to the excitation of internal gravity waves of different periods and the rise in their amplitude [29, 30].

From this point of view, we consider a sequence of altitude temperature profiles presented in Fig. 3. In our opinion, such dynamics of the profiles can indicate both the instability development and a certain turbulization of the medium. Thus, the presence of the temperature gradient required for the instability development (the profiles for 11:45 and 12:05 MSK, Fig. 3*a*) leads to this effect both in accordance with the Richardson criterion and, possibly, due to the shear of the horizontal velocity and the temporal variation of the medium characteristics. As a result, a sufficiently smooth profile of the temperature transforms to the profile presented for the sessions at 12:55 and 13:05 MSK in Fig. 3*b*. Recall that these data were obtained by averaging over a 10-min interval. The next two temperature profiles obtained for the sessions at 14:25 and 14:45 MSK and shown in Fig. 3*c* apparently correspond to the conditions in Fig. 3*a*. Namely, the "quiet" temperature profile can be recovered as a result of the ionospheric state variation at the altitudes of the lower thermosphere, i.e., due to variations in the electron-density profile, horizontal and vertical velocities, and other parameters. It follows from Fig. 3 that this temperature profile has the same gradient $\partial T/\partial z$ as that required for the instability development, which takes place in some time, as is displayed in Fig. 3*d* for the sessions at 16:35 and 16:45 MSK. Note that a similar pattern with the transition from the "quiet" to "perturbed" profile was also recorded in the observations of September 24, 2007 in Figs. 4*a* and 4*b*.

We also note that for the vertical-velocity shears $\partial u_0/\partial z$ exceeding the value $\partial u_0/\partial z = 2\omega_g \approx 3.4 \cdot 10^{-2}$ s^{-1}, there is a high probability for the dynamic instability development and the atmospheric turbulization. Such gradients $\partial u_0/\partial z$ were observed in the experiments (see, e.g., [31–33]).

The possibility that the instability can develop at the altitudes of the E region is indirectly indicated by the fact that the variations in characteristics of the scattered signal, its amplitude and relaxation time increase in certain periods of time. Moreover, the turbulent velocity values determined, according to Eq. (4), by measurements at two frequencies in September 24, 2007 turned out to be high enough and reached 7–10 m/s at altitudes of 90–95 km. Thus, using the results of studying the dynamics of the lower ionosphere by the method of resonant scattering of radio waves by artificial periodic irregularities, both the wave and turbulent motions, which led to the temporal variations of the altitude temperature profile of the neutral component, were recorded.

5. CONCLUSIONS

Uring the method of resonant scattering of radio waves by artificial periodic irregularities, we determined the spatio-temporal dependencies of the neutral-atmosphere parameters, such as temperatures, densities, and vertical velocities, including the turbulent motion, at the altitudes of the mesosphere — lower thermosphere. Perturbations of these parameters, which are often unstable, are observed in many cases. They can be stipulated by the propagation of internal gravity waves, as well as the violation of the hydrodynamic stability conditions. Criteria for the development of hydrodynamic instabilities in this altitude interval, which are put into correspondence with the experimental results, are presented. The following conclusions have been drawn. 1) The propagation of internal gravity waves with periods 30–60 min in a stably stratified medium does lead to its instability. Spectral analysis of the temporal variations of the amplitude and relaxation time of the signal backscattered by periodic artificial irregularities has shown that the internal gravity waves with such periods have the largest intensity in the spectrum, and they were stably recorded. 2) The reason for the instability occurrence can be the negative temperature gradient of the atmosphere. The criterion $\partial T/\partial z < -(10\text{—}12)$ K/km is a sufficient condition for the instability development.

Negative temperature gradients were observed many times in the experiments, reaching −20 K/km, and the atmospheric-parameter disturbances manifested by altitude–time variations were recorded in the subsequent instants of time. 3) The reason for the instability in an isothermal atmosphere can also be the shear of the horizontal velocity of the medium, $\partial u_0/\partial z$, which exceeds the value $\partial u_0/\partial z = 2\omega_g \approx 3.4 \cdot 10^{-2}$ s^{-1}. Such wind shears were observed many times in different experiments, and they could lead to the shear hydrodynamic instability. 4) Due to the excitation of internal gravity waves with different periods and the rise in their temperature, the turbulization of the medium can be expected. Indeed, elevated values of the turbulent velocity up to 7–10 m/s at altitudes 90–95 km for the turbopause altitude 100–105 km were obtained in September 24, 2007. Thus, the theoretical estimates of the criteria of the hydrodynamic instabily development, which we made in this paper, and their comparison with the development of spatio-temporal variations of the observed atmospheric parameters and characteristics of the wave and turbulent motions confirm the conclusion that the instabilities and atmospheric waves tangibly affect the dynamics of the mesophere — lower thermosphere in the altitude interval 90–120 km.

This work was supported in part by the Russian Foundation for Basic Research (project Nos. 08–02–97036 and 09–05–00450).

REFERENCES

1. V. V. Koshelev, N. N. Klimov, and N. A. Sutyrin, *Aeronomy of the Mesosphere and Lower Thermosphere* [in Russian], Nauka, Moscow (1983).
2. N. N. Shefov, A. I. Semenov, and V. Yu. Khomin, *Radiation of the Upper Atmosphere* [in Russian], Geos, Moscow (2006).
3. E. A. Benediktov, V. V. Belikovich, A. V. Tolmacheva, and N. V. Bakhmet'yeva, *Ionospheric Research by Means of Artificial Periodic Irregularities* [in Russian], Inst. Appl. Phys., Russ. Acad. Sci., Nizhny Novgorod (1999).
4. N. V. Bakhmet'eva, V. V. Belikovich, G. I. Grigor'ev, and A. V. Tolmacheva, *Radiophys. Quantum Electron.*, **45**, No. 3, 211 (2002).
5. V. V. Belikovich, E. A. Benediktov, A. V. Tolmacheva, and N. V. Bakhmet'eva, *Ionospheric Research by Means of Artificial Periodic Irregularities*, Katlenburg–Lindau, Copernicus GmbH (2002).
6. V. V. Belikovich, N. V. Bakhmet'eva, E. E. Kalinina, and A. V. Tolmacheva, *Radiophys. Quantum Electron.*, **49**, No. 9, 669 (2006).
7. N. V. Bakhmet'eva, V. V. Belikovich, and A. V. Tolmacheva, in: *Proc. XXII Russian Conf. on Propagation of Radio Waves, 22–26 September, 2008, Rostov-on-Don, Loo* [in Russian], Vol. 2, p.İ29.
8. A. V. Tolmacheva, V. V. Belikovich, and E. E. Kalinina, *Geomag. Aeron.*, **49**, No. 2, 239 (2009).
9. N. V. Bakhmet'eva, V. V. Belikovich, E. A. Benediktov, et al., *Radio Sci.*, **33**, No. 3, 583 (1998).
10. E. A. Benediktov, V. V. Belikovich, N. V. Bakhmet'eva, and A. V. Tolmacheva, *Radiophys. Quantum Electron.*, **45**, No. 5, 343 (2002).
11. E. A. Benediktov, V. V. Belikovich, Yu. A. Grebnev, and A. V. Tolmacheva, *Geomagn. Aéron.*, **33**, No. 5, 170 (1993).
12. V. V. Belikovich, E. A. Benediktov, and A. V. Tolmacheva, *Izv., Atmos. Oceanic Phys.*, **38**, No. 1, 89 (2002).
13. V. V. Belikovich and A. V. Tolmacheva, *Int. J. Geomag. Aeron.*, **5**, GI1008 (2004).
14. B. N. Gershman, *Dynamics of the Ionospheric Plasma* [in Russian], Nauka, Moscow (1974).
15. N. V. Bakhmet'eva, V. V. Belikovich, M. N. Egerev, and A. V. Tolmacheva, *Radiophys. Quantum Electron.*, **53**, No. 3, 69 (2010).

16. L. M. Brekhovskikh and V. V. Goncharov, *Introduction to the Mechanics of Continuous Media* [in Russian], Nauka, Moscow (1982).
17. G. I. Grigor'ev and O. N. Savina, *Radiophys. Quantum Electron.*, **45**, No. 8, 606 (2002).
18. C. Chandrasekhar, *Hydrodynamic and Hydromagnetic Stability.* Oxford University Press, London (1961).
19. L. A. Dikiy, *Hydrodynamic Stability and Dynamics of the Atmosphere* [in Russian], Gidrometeoizdat, Leningrad (1976).
20. Yu. Z. Miropol'sky, *Dynamics of the Internal Gravity Waves in the Ocean* [in Russian], Gidrometeoizdat, Moscow (1981).
21. G. I. Grigor'ev, "Propagation of acoutic-gravity waves in nonstationarily moving media: a review" [in Russian], Preprint No. 482, Radiophysical Research Institute, Nizhny Novgorod (2005).
22. C. Sridharam, S. Sathishkumar, and N. S. Gurubara, *Ann. Geophys.*, **26**, 3781 (2008).
23. B. R. Williams, D. C. Fritts, C. Y. She, and R. A. Goldberg, *Ann. Geophys.*, **24**, 1199 (2006).
24. N. P. Shakina, *Hydrodynamic Instability in the Atmosphere* [in Russian], Gidrometeoizdat, Leningrad (1990).
25. J. W. Miles,*J. Fluid Mech.*, **10**, 496 (1961).
26. M. V. Kurgansky, *Izv. Akad. Nauk, Fiz. Atm. Okeana*, **15**, No. 10, 1911 (1979).
27. S. P. Kshevetskii and N. M. Gavrilov, *Geomag. Aeron.*, **43**, No. 1, 69 (2003).
28. A. B. Shvartsburg, *Phys. Usp.*, **48**, No. 8, 797 (2005).
29. C. O. Hines, in: W. L. Webb, ed., *Thermospheric Circulation*, Cambridge, MA, MIT Press (1972).
30. E. E. Gossard and W. H. Hook, *Waves in the Atmosphere*, Elsevier, The Netherlands (1975)
31. Y.-Fu. Wu and H. V. Widdel, *J. Atm. Terr. Phys.*, **54**, No. 2, 143 (1992).
32. É. S. Kazimirovsky and V. D. Kokourov, *Motions in the Ionosphere* [in Russian], Nauka (Siberian Branch), Novosibirsk (1979).
33. Yu. I. Portnyagin and K. Sprenger, eds., *Wind Measurements at* 90–100 *km Altitudes by Means of Ground-Based Techniques* [in Russian], Gidrometeoizdat, Leningrad (1978).